© Pol J Radiol 2023; 88: e124-e134
DOI: https://doi.org/10.5114/pjr.2023.125981

Received: 11.09.2022
Accepted: 21.11.2022
Published: 03.03.2023

Polish Journal of Radiology

http://www.polradiol.com

Original paper

"Keep it simple – a lesson from COVID-19": highlighting the utility of chest X-rays in ARDS-associated illnesses through the Zonal Scoring System

Anna Rachel Menezes[A,B,C,D,E,F], Arun George[A,B,C,D,E,F], Linda Ann Joseph[B,C,D,E,F], Bimal Saju[B,C,D,E,F], Athul Varghese Kurian[A,B,F]

St. John's Medical College, Bengaluru, Karantaka, India

Abstract

Purpose: The post-pandemic era calls for appropriate literature on chest X-ray score cut-offs, enabling swift categorization and faster radiological reporting of patients with acute respiratory distress syndrome (ARDS)-like illnesses, hence prompting healthcare equity in low-resource centres where extortionate modalities of imaging such as computed tomography (CT) are unavailable. In this study, we aim to bridge the literature gap using the versatile zonal scoring system.

Material and methods: This retrospective cohort study uses data from 751 COVID-19 RT-PCR+ patients. Concordant chest radiograph (CXR) scores were reported, and inter-rater reliability was measured using kappa indices. receiver operating characteristic curves were used to establish cut-off scores for the outcomes of interest: mild or severe disease, admission to an intensive care unit (ICU), and intubation. Categorical data were expressed using means and percentages, and χ^2 or *t*-tests were used for comparison at an α level of 0.05. Unadjusted odds ratios for each outcome of interest vs. CXR score and comorbidity were then calculated using binary logistic regression.

Results: CXR findings included infiltrates (46.07%), pleural effusions (7.05%), consolidation and fibrosis (4.43%), pneumothoraces (2.71%), and cardiomegaly (2.26%). Most patients had an index CXR score of 0 (54.19%). The index cut-off score of ≤ 1 (82.95, 81.68) was established for mild disease, ≥ 4 for severe disease (85.71, 83.99), ≥ 3 for ICU admission (86.90, 71.91), and ≥ 4 for intubation (87.61, 72.90). Hypertension, type 2 diabetes mellitus, hypothyroidism, history of ischaemic heart disease, and history of tuberculosis were independent risk factors for a high CXR index score, intubation, and ICU admission.

Conclusions: CXR scores can be effectively used in low-resource settings for triaging patients, maintaining records, and disease prognostication.

Key words: chest X-ray scores, COVID-19, ARDS, ICU admission, intubation.

Introduction

The severe acute respiratory syndrome coronavirus-2 (SARS-CoV-2), a non-enveloped RNA virus, wreaked havoc in the short span of 3 years during its evolution from an outbreak in Wuhan, China to a widespread universal pandemic [1]. As of July 2022, the virus had evolved into 5 different key species and tallied over 5.6 million deaths globally [2]. To ease triaging of patients the World Health Organization (WHO) categorized patients into mild, moderate, and severe disease based on clinical features of dyspnoea, room air saturation, fever,

Correspondence address:
Anna Rachel Menezes, St. John's Medical College, Sarjapur – Marathahalli Rd, beside Bank Of Baroda, John Nagar, Koramangala, Bengaluru, Karnataka 560034, India, e-mail: annamenez97@gmail.com

Authors' contribution:
A Study design · **B** Data collection · **C** Statistical analysis · **D** Data interpretation · **E** Manuscript preparation · **F** Literature search · **G** Funds collection

and the number of respiratory cycles per minute. The prevalence of each category in the year 2021 was reported to be 81%, 14%, and 5%, respectively [3]. Due to the stativity of newly diagnosed coronavirus disease (COVID) cases in the past few months, epidemiologists are considering its transformation into an endemic disease, although they continue to urge that policymakers be wary of the harmful effects of the virus [4].

During the pandemic, multiple radiological methods were used to aid in diagnosing and categorizing patients. At the start of it, attempts were made to evaluate the usage of portable ultrasound imaging (US), and features including B-lines (100%), consolidation (67.9%), and thickened pleural lines (60.7%) were found in most patients affected by the disease [5]. The 2 latter features also pointed toward an increased severity of COVID-19 infection [5]. The usage of US in COVID-19 was limited due to the necessity of trained professionals for accurate results and its limitations to be used swiftly in an intensive care unit (ICU) setting. Furthermore, in the course of the pandemic, computed tomography (CT) was used as a mainstay for both radiological diagnosis and disease prognostication due to its high sensitivity [6]. CT findings included bilateral peripheral ground-glass opacities (GGOs) (88%), focal consolidation (31.8%), linear opacities, and crazy paving pattern, all of which were highest during days 6-12 of the disease [7-9]. During the pandemic, the literature focused on the evaluation of CT in grading the severity of the illness, and innumerable scores were curated to validate its diagnostic and prognostic value, while the affordable and readily available chest radiograph (CXR) was overshadowed. Although, via the ResNet-18 imaging technique, Benmalek *et al.* showed that CXRs have a comparable sensitivity in detecting COVID-19 (94.9%) with CT (99%) [10]. The above was further supported in a study by Sverzellati *et al.* in 2021, proposing that first-line CXRs and contiguous high-resolution CTs provide the best radiological assessment for COVID-19 [11]. Even though CT was shown to have a higher predictive value than CXR, its utility was partly limited by: a) the need for continuous decontamination to ensure adequate infection control in the CT suite; b) the need for trained radiologists to correctly interpret results; and c) decreased utility in low resource settings due to the implications of cost and equipment [12,13]. These features contribute to the increased need for literature on the utility of CXR in identifying and grading the severity of respiratory illnesses, such as COVID-19, especially in developing countries like India, where it can be performed relatively inexpensively.

Features of COVID-19 on CXRs range from consolidation opacities (81.3%) to reticular interstitial thickening (39.9%), predominantly in the lower zone [8,10]. In contrast to CT, only a handful of scores have been used to categorize the severity of lung involvement in CXR, including the Brixia score, the RALE (Radiographic Assessment of Lung Edema), and the zonal scoring system developed by Toussie *et al.* in May 2020 [14-16]. The RALE scoring system divides each lung into 2 quadrants and attributes a different score for consolidation and opacity, with a maximum score of 48 [15]. It also requires trained radiologists for appropriate execution, unlike the Brixia or the zonal scoring, which divides the lung into 6 zones. The Brixia score assigns a score of 1 for interstitial infiltrates and 2 or 3 for a combination of interstitial and alveolar infiltrates with interstitial or alveolar predominance, respectively, adding up to a maximum possible score of 18 [16]. The zonal scoring system developed by Toussie *et al.* used only a binary score of 0 or 1 depending on the presence of opacity in each zone [14]. In the study, Toussie *et al.* opined that CXR severity scores (CXR SS) of > 2 were an independent predictor for admission, and scores of > 3 were an independent predictor of intubation [14]. Due to its simplicity, high predictive value, i.e. odds ratio (OR) of 4.7 for intubation, and lack of the need for additional analytical software, we chose the zonal scoring system to perform our study.

The implications of using the index CXR, i.e. the first CXR during admission in the categorization and prognosis of patients with acute respiratory distress syndrome (ARDS) remain largely unknown, particularly in a low-resource setting. A study conducted in the Emergency Department of a tertiary care hospital in the South Asian region using a simplified version of RALE's established that initial and highest scores are independent predictors for admission and intubation, in agreement with the premiere study performed at Mount Sinai Hospital, New York [13,14]. Nevertheless, even after a thorough review of literature, knowledge on appropriate cut-offs for categorization of patients according to serviceable CXR scores and the effect of comorbidities apart from hypertension (HTN), diabetes mellitus (T2DM), and asthma on them is still lacking. In this study, we aimed to bridge the unmet need for literature on CXR scores in a background of COVID-19 and invigorate its further use in low-resource centres in the Middle-East and South-East Asian sub-continents for oncoming waves of similar or novel respiratory illnesses.

Material and methods

Study design and location

A retrospective cohort study was conducted using data from 751 patients admitted to St. John's Medical College Hospital, a tertiary and referral health care centre in South India. The study duration was from April to December 2021, including patients admitted during the second wave of the pandemic in India.

All patients between 18 and 80 years of age with positive COVID-19 real-time polymerase chain reaction (RT-PCR) reports at the time of admission were considered for the study. The age criteria were set to reduce con-

founding factors of chronic lung disease and heart failure [14]. Patients with repeated medical records, lack of RT-PCR-positive reports or index CXR, and incomplete clinical data were excluded (Figure 1).

Ethical approval

Ethical approval and permission for waiver of consent were obtained from the Institutional Ethics Committee, reference number 311/2021. Consent was waivered with the precept that all subjects were admitted to the hospital, and only routine data, delinked from patient identifiers collected during the hospital stay, were used.

Data collection

Data were collected using electronic medical records and a picture archiving and communicating system (PACS) as follows:

Clinical data

Demographic data, including age, sex, and comorbidities like HTN, T2DM, asthma, chronic kidney disease (CKD), etc. were tabulated. All patients were retrospectively followed up for features of mild, moderate, or severe COVID, according to WHO criteria, as follows [17]:

- mild: temperatures > 37.5° and cough with no dyspnoea;
- moderate: features of lower respiratory tract infection (LRTI), i.e. temperature > 37.5°, cough, and dyspnoea with room air saturation ≥ 94%;
- severe-critical: features of LRTI with room air saturation < 94% or a respiratory rate greater than 30 cycles per minute, with or without respiratory failure, septic shock, or multiple organ dysfunction.

In addition, patients were retrospectively followed up for ICU admission, ventilation, discharge, and mortality. Data were collected by medical students (L.A, B.S) who were blinded to the radiological features of the patient.

Imaging data

All CXRs were performed using a portable hybrid analogue CXR machine with a digitizer: Siemens (Germany) Multimobil 2.5, in the respective COVID-19-positive isolation wards, intensive treatment units (ITU), and ICUs. Two junior residents from the Department of Radiology with experience in chest imaging calculated the CXR scores for each patient independently. The 2 residents were individually trained on CXR score assessment, and the study began only after data saturation (1-week ± 3 days). The readings were further reviewed by a senior radiologist with over 20 years of experience. Only concordant findings were analysed. All 3 readers were blinded to patient history apart from COVID-19 positivity to truncate bias.

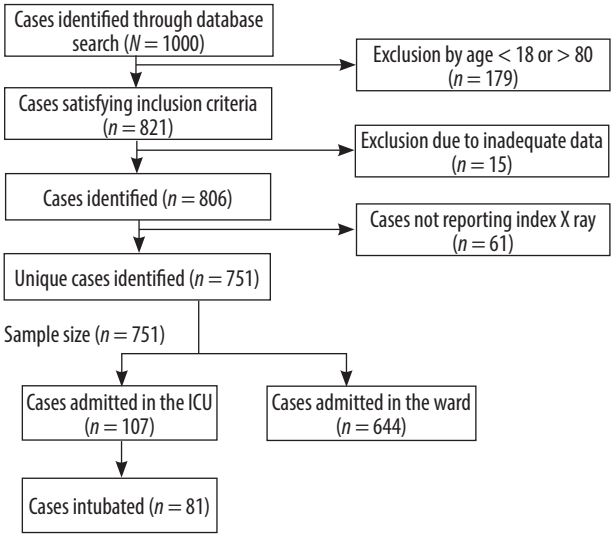

Figure 1. Flow diagram of the retrospective cohort study

Imaging analysis

CXR scores of the first CXR on admission (index CXR) were calculated using the zonal scoring system. Each lung was divided into 3 regions as follows [14]:

- zone 1: extending from costophrenic sulcus to inferior hilar marking;
- zone 2: extending from inferior hilar to superior hilar marking;
- zone 3: extending from superior hilar marking to apices of lung.

A score of 1 was allotted to a zone with any opacity, and a score of 0 was assigned to a zone without any opacity. The total score was calculated and reported, with a minimum possible score of 0 and a maximum score of 6.

Figure 2 shows a portable CXR taken on a 45-year-old patient with no comorbidities on admission. Rotation of the lungs due to inadequate positioning of the patient is present. No opacities are visualized in any zones tabulating the CXR score to 0. The patient was treated as a mild COVID-19 case and discharged on Day 10 of admission per the hospital protocol for COVID-19 isolation.

Portable Hybrid Analogue CXR images taken on patients from the COVID-19-positive isolation ward, ICU, and ITU with descriptors for calculation and example scores of each CXR.

Statistical analysis

IBM Statistical Package for the Social Sciences (IBM SPSS 26) (Chicago, USA) and Python 3.9 (CWI, Netherlands) were used for statistical analysis. Values were considered significant at $p < 0.05$. Confidence intervals are reported at 95%.

Descriptive statistics

Categorical data are represented using means and percentages. *P*-value was determined using 2-tailed nonpara-

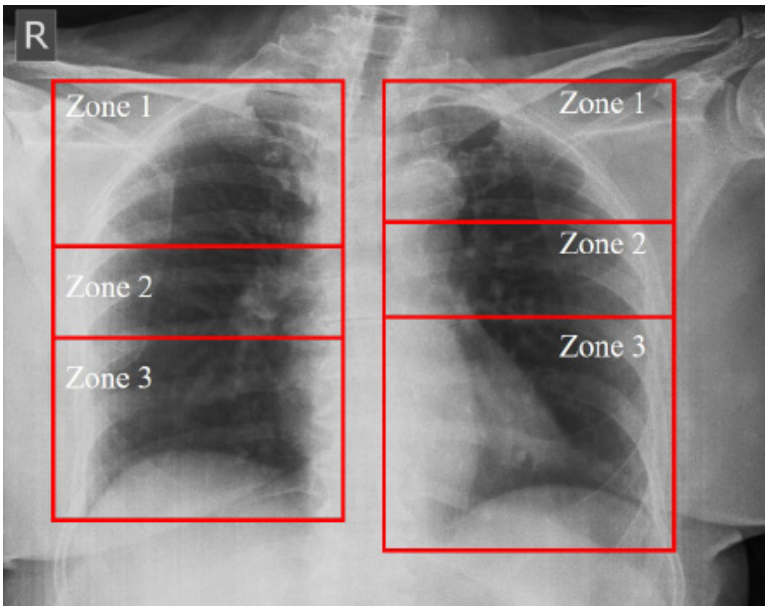

Figure 2. Division of the lung into zones for calculation of chest severity score

metric tests, i.e. χ^2 test and *t*-test, used to compare means in a distribution-free pattern. Odds ratios were calculated using binary logistic regression.

Inter-rater reliability

Cohen's κ was used to assess agreement in radiological scores among the 3 radiologists using the first 250 CXRs. Calculations were based on the sum of zonal scores

Receiver operating characteristic curve (ROC) analysis

ROC curves were drawn for each outcome of interest, i.e. mild and severe COVID-19, ICU admission, and ventilation using Python 3.9. The cut-off value was determined with the highest true-positive rate – (false-positive rate). The area under the curve, sensitivity, and specificity were calculated for each cut-off score. Additionally, the Youden Index (YI) for each cut-off was calculated using SPSS 26, and the cut-off score with the highest YI was confirmed at an acceptable level of > 50% only.

Correlational statistics and effect of comorbidities

The Mann-Whitney *U* test was used to compare the index CXR scores (ICXRSs) in the background of each comorbidity. Logistic regression was used to calculate the unadjusted odds ratio of each variable and correlate it to the categorical outcomes of an ICXRS of ≥ 4, admission to ICU, and intubation.

Results

A total of 751 patients were admitted to the ICU, ITU, and the ward, with 63.24% of patients being male. The median age of the patients was 49 years, with an interquartile range of 32 to 78 years. 58.58% of patients were categorized into the WHO clinical category of mild, 16.2% of patients – moderate, and 25.1% – severe, during the hospital stay. The higher proportion of severe patients compared to WHO demographics was attributed to Berkson's bias that the study was conducted in a referral hospital during the second wave of the COVID-19 pandemic, and only admitted patients were evaluated [18]. Patient demographics are related to categorical outcomes in Table 1. A total of 107 were admitted to the ICU (14.24%), of whom 81 were intubated. Sixty-three (8.38%) deaths were tabulated in total. There was no statistical significance between mean age or sex ICXRS of ≥ 4 at admission. Out of 751 admitted patients, 6 were discharged against medical advice, all of whom had ICXRS ≤ 1. Other outcomes of interest, i.e. ICU admission, intubation, and mortality, had a significant association with ICXRS ≥ 4, as portrayed in Table 1.

Table 2 describes the comorbidity and CXR score demographics of the sample size. The most common comorbidity was diabetes mellitus (T2DM) (40.6%) followed by hypertension (HTN) (37.94%), dyslipidaemia (20.10%), obesity (18.97%), obstructive sleep Apnoea (OSA) (8.25%), history of coronary artery disease (CAD) (7.88%), and hypothyroidism (5.59%). Other frequent comorbidities included chronic kidney disease (CKD) (4.79%), asthma (4.39%), and history of cerebral vascular disease (CVD) (2.39%).

Chest X-ray findings

CXR findings ranged from interstitial and alveolar infiltrates (46.07%), pleural effusions (7.05%), consolidation and fibrosis (4.43%), pneumothoraces (2.71%), and cardiomegaly (2.26%). Among the 53 patients with pleural effusions,

27 (48.14%) had a bilateral effusion, 20 (37.70%) had a left-sided pleural effusion, and the 11 remaining patients (14.16%) had a right-sided effusion. Pneumothoraces had a statistically significant association with ICU admission ($p = 0.031$), with 17 out of 20 patients with pneumothoraces eventually being admitted to the ICU or having been referred from other tertiary centres due to the need for intubation. Cardiomegaly had a significant association with hypertension ($p < 0.001$).

The κ coefficient of the 3 radiologists was calculated to be 0.82 ($p < 0.05$), showing excellent inter-rater reliability.

Among the 751 CXRs evaluated, the majority of 407 had an ICXRS of 0 (54.19%). The mean ICXRS was 1.9280 with a standard deviation of 2.3426. A total of 17 patients had an ICXRS of 1 (2.26%), 55 (7.32%) – 2, 22 (2.92%) – 3, 114 (15.15%) – 4, 29 (3.86%) – 5, and 107 (14.24) had a score of 6.

Receiver operating characteristic curve analysis

Receiver operating characteristic curves were drawn to establish cut-off IXCRSs for categorization into mild and severe diseases, as shown in Figures 3A and 3B. Patients

Table 1. Patient demographics and categorical outcomes related to chest X-ray (CXR) score

Variable	Total no. of patients ($N = 751$)	Index CXR score ≤ 1 ($n = 422$)	Index CXR score ≥ 4 ($n = 252$)	*p*-value
Median age, years (SD)	49 (16.63)	49 (14.21)	51 (18.15)	0.11
Male sex, *n* (%)	475 (63.24)	211 (44.42)	156 (32.84)	0.587
Admitted to ICU, *n* (%)	107 (14.24)	11 (10.28)	89 (83.17)	< 0.00001
Intubation, *n* (%)	81 (10.78)	5 (6.17)	71 (87.65)	< 0.00001
Admitted to ITU/ward, *n* (%)	644 (85.75)	411 (63.81)	163 (25.31)	< 0.00001
Discharged against medical advice, *n* (%)	6 (0.79)	6 (100)	0	–
Deaths, *n* (%)	63 (4.44)	2 (3.17)	51 (80.9)	< 0.00001
WHO clinical category, *n* (%)				
Mild	440 (58.58)	365 (82.95)	39 (8.86)	< 0.00001
Moderate	122 (16.2)	59 (48.36)	51 (41.80)	0.035
Severe	189 (25.1)	16 (8.4)	162 (85.71)	< 0.00001

Table 2. Comorbidity demographics concerning chest X-ray (CXR) score

Comorbidity	Total no. of patients ($N = 751$), *n* (%)	CXR ≤ 1 ($n = 422$)	CXR ≥ 4 ($n = 252$)	*p*-value
Hypertension	285 (37.94)	135	122	0.00002
Diabetes mellitus	305 (40.6)	120	141	< 0.0001
Asthma	33 (4.39)	22	8	0.246
Hypothyroidism	42 (5.59)	23	15	0.7603
Hyperthyroidism	4 (0.53)	2	2	0.4849
Chronic kidney disease	36 (4.79)	11	20	0.0041
Coronary artery disease	60 (7.98)	20	37	< 0.00001
Obesity	120 (15.97)	19	98	< 0.00001
Dyslipidaemia	151 (20.10)	21	96	< 0.00001
Obstructive sleep apnoea	62 (8.25)	6	42	< 0.00001
Cerebral vascular disease	18 (2.39)	15	3	0.1245
Systemic lupus erythematosus	2 (0.26)	0	2	0.0462
History of tuberculosis	3 (0.039)	0	3	0.0145
Chronic hepatitis B	1 (0.013)	0	1	0.1590
Rheumatic heart disease	2 (0.26)	1	1	0.6218
Malignancy	4 (0.53)	4	0	0.1541
Myasthenia gravis	5 (0.66)	1	3	0.2086
Homocysteinaemia	2 (0.26)	1	0	0.3142

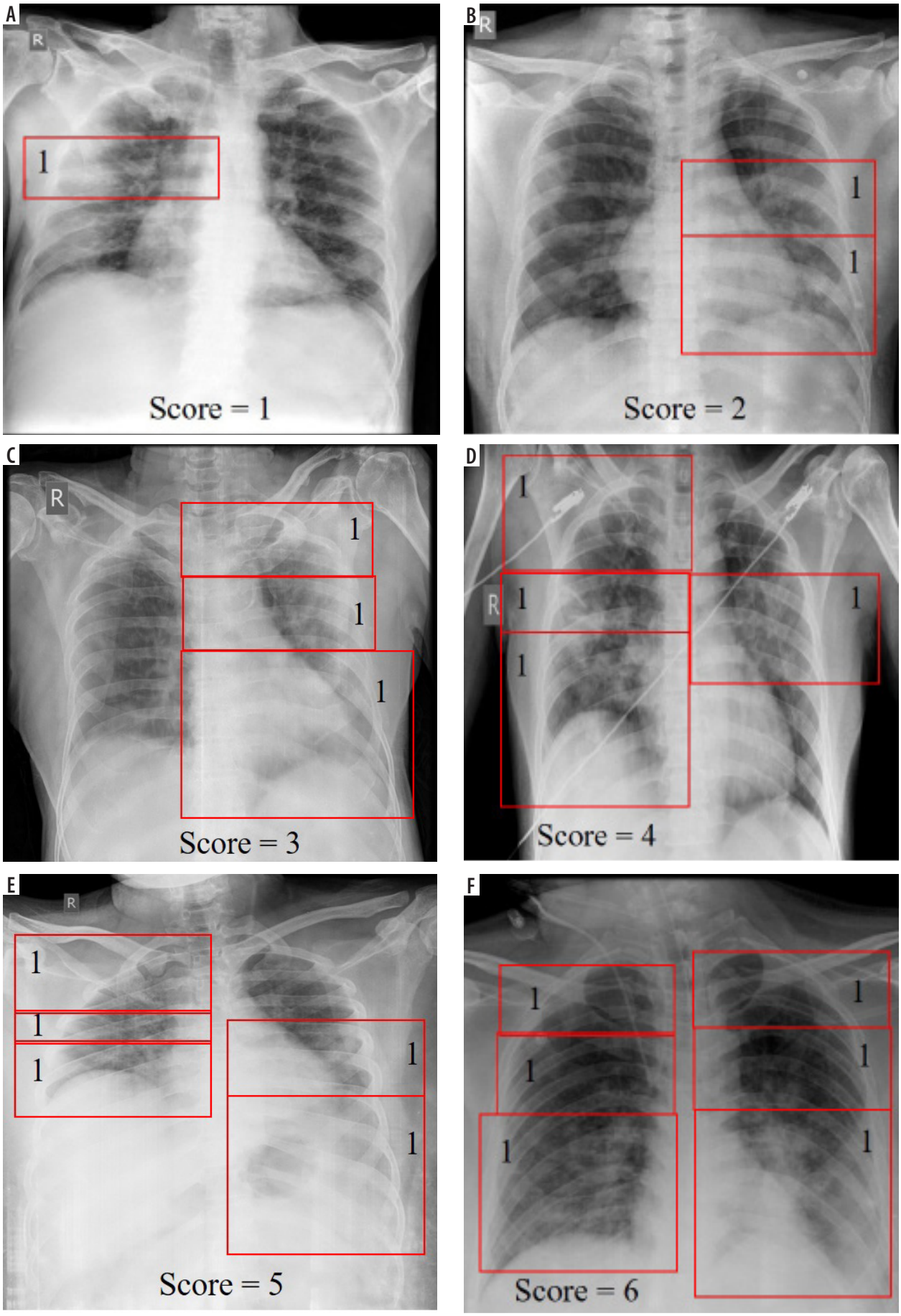

Figure 3. Method of calculation of CXR scores with examples of scores 1-6

with ICXRS falling between mild and severe disease cut-offs were classified as moderate.

Figure 3A shows the ROC curve for the categorization of patients as mild. The area under the curve is 0.864, confidence interval (CI) = 0.835-0.892 ,with a standard error (SE) of 0.015, $p < 0.0001$. Table 3A shows the true positive rate (TPR) and false positive rate (FPR), i.e. (1-specificity) for each cut-off point in the ROC curve. The cut-off ICXRS for mild disease was established at a score of ≤ 1 with a sensitivity of 82.95% and a specificity of 81.69%.

Figure 3B depicts an ROC curve for establishing a cut-off ICXRS for severe disease. The area under the curve is 0.885 (CI = 0.856-0.914, SE = 0.015, $p < 0.0001$). Table 4A shows TPR and FPR for each cut-off point in the ROC curve 3B. The cut-off ICXRS was a score of ≥ 4 at a sensitivity of 85.71% and a specificity of 83.99%.

As portrayed in Figures 4C, D and Tables 3C and D, respectively, cut-off ICXRS for ICU admission and intubation were demarcated at ≥ 3 and ≥ 4. The sensitivity of the cut-off was 86.90% and specificity was 71.91% for predicting ICU admission and 87.61% and 72.90%, respectively, for intubation. The area under the ROC curve in Figure 4C (ICU admission) was 0.826 (SE = 0.021, CI = 0.785-0.967, $p < 0.0001$) and Figure 4D (intubation) was 0.83 (SE = 0.020, CI = 0.796-0.873, $p < 0.0001$).

Correlational analysis depicting the effect of comorbidities on ICXRS

Comorbidities with a statistically significant prevalence in the sample size and respective CXR scores were analysed. Using the Mann-Whitney *U* test, HTN had an

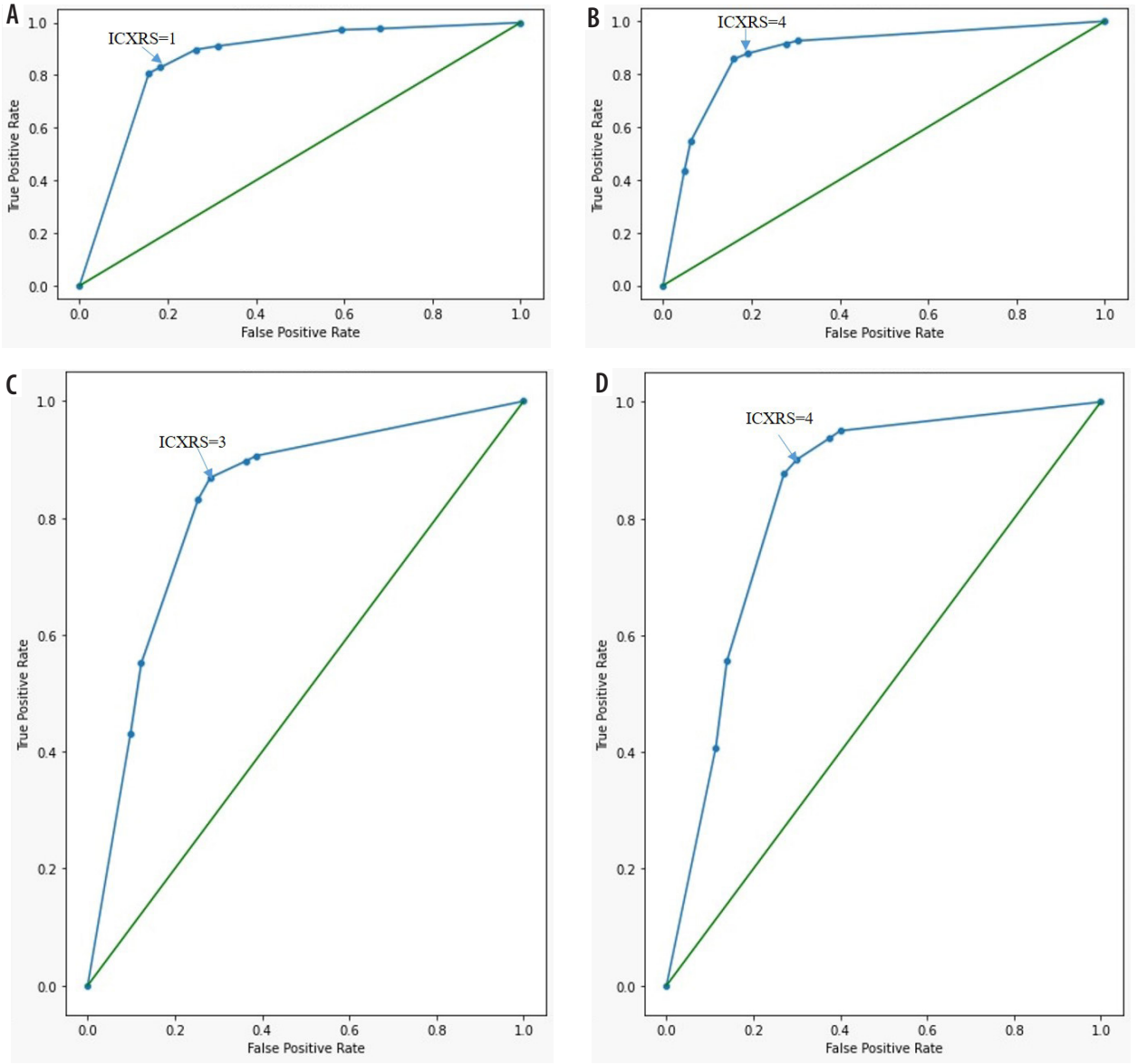

Figure 4. **A**) Receiver operating characteristic curves establishing cut-off scores for mild disease. **B**) Receiver operating characteristic curves establishing cut-off scores for severe disease. **C**) Receiver operating characteristic curves establishing cut-off scores for ICU admission. **D**) Receiver operating characteristic curves establishing cut-off scores for intubation

Table 3.

A. TPR and FPR for ICXRS cut-off on ROC curve of Figure 4A (mild disease)

Cut-off CXRS	True positive rate (TPR)	False positive rate (FPR)	(TPR-FPR)
0	0.809	0.1675	0.6415
1	0.8295	0.1832	0.6463
2	0.8977	0.2633	0.6344
3	0.9113	0.3151	0.5962
4	0.9727	0.5948	0.3779
5	0.9772	0.6816	0.2956
6	1	1	0

B. TPR and FPR for ICXRS cut-off on ROC curve of Figure 4B (severe disease)

Cut-off CXRS	True positive rate (TPR)	False positive rate (FPR)	(TPR-FPR)
0	1	1	0
1	0.9259	0.3042	0.6217
2	0.9153	0.2775	0.6378
3	0.8783	0.1921	0.6862
4	0.8571	0.1601	0.697
5	0.5449	0.0622	0.4827
6	0.4338	0.048	0.3858

C. Associated true positive rate and false positive rate for each cut-off on the ROC curve of Figure 3C (ICU admission)

Cut-off CXRS	True positive rate (TPR)	False positive rate (FPR)	(TPR-FPR)
0	1	1	0
1	0.906	0.388	0.518
2	0.897	0.361	0.536
3	0.869	0.281	0.588
4	0.831	0.253	0.578
5	0.551	0.112	0.439
6	0.429	0.09	0.339

D. Associated true positive rate and false positive rate for each cut-off on the ROC curve of Figure 4D

Cut-off CXRS	True positive rate (TPR)	False positive rate (FPR)	(TPR-FPR)
0	1	1	0
1	0.905	0.4	0.505
2	0.938	0.376	0.562
3	0.901	0.3	0.601
4	0.876	0.27	0.606
5	0.555	0.138	0.417
6	0.407	0.113	0.294

unadjusted odds ratio (uOR) of 1.172, 2.498, and 2.339 for ICXRS ≥ 4, ICU admission, and intubation, respectively. As tabulated in Table 4 (A-C), other comorbidities with a uOR of > 1 for outcomes of interest were T2DM, dyslipidaemia, obesity, OSA, history of CAD, CKD, and CVD. The most substantial independent risk factors for a higher ICXRS were a previous history of treated tuberculosis ($p = 0.165$), OSA, obesity, T2DM, and HTN ($p < 0.05$), and the highest uORs for ICU admission and ventilation were computed for obesity, HTN, and OSA.

Table 4.

A. Odds ratios for categorical outcomes of CXR score > 4

Comorbidity	Unadjusted odds ratio (uOR)	Confidence interval	Standard error	*p*-value
Hypertension	1.172	1.100-1.243	0.032	< 0.0001
Diabetes mellitus	1.267	1.188-1.351	0.033	< 0.0001
Dyslipidaemia	1.105	1.046-1.252	0.026	< 0.0001
Obesity	1.317	1.261-1.482	0.031	< 0.0001
Obstructive sleep apnoea	1.413	1.363-1.514	0.022	< 0.0001
History of coronary artery disease	1.135	1.091-1.263	0.070	0.021
Chronic kidney disease	1.251	1.092-1.434	0.070	< 0.0001
History of treated tuberculosis	1.426	0.863-2.354	0.256	0.165

B. Odds ratios for categorical outcomes of ICU admission

Comorbidity	Unadjusted odds ratio (uOR)	Confidence interval	*p*-value
Hypertension	2.498	1.649-3.786	< 0.0001
Diabetes mellitus	1.512	1.228-1.861	< 0.005
Dyslipidaemia	1.363	1.143-1.465	< 0.0001
Obesity	2.468	1.561-3.588	< 0.0001
Obstructive sleep apnoea	1.984	1.344-2.543	< 0.0001
History of coronary artery disease	1.149	1.054-1.253	0.002
Chronic kidney disease	1.371	1.194-1.577	0.071
History of treated tuberculosis	1.311	0.988-1.434	0.505

C. Odds ratios for categorical outcomes of intubation

Comorbidity	Unadjusted odd's ratio (uOR)	Confidence interval	*p*-value
Hypertension	2.339	1.463-3.740	< 0.0001
Diabetes mellitus	1.394	1.104-1.761	< 0.005
Dyslipidaemia	1.263	1.114-1.431	< 0.0001
Obesity	1.499	1.241-1.765	< 0.0001
Obstructive sleep apnoea	2.116	1.812-2.984	< 0.005
History of coronary artery disease	1.092	0.985-1.211	0.095
Chronic kidney disease	1.206	1.023-1.422	0.026
History of treated tuberculosis	1.003	0.758-1.021	0.665

Discussion

In a post-pandemic era, where additional efforts are being made to strengthen healthcare preparedness for further waves and novel respiratory illnesses, there is a critical need in developing countries like India to use remunerative imaging techniques such as CXR to triage patients [19,20]. In our study, we adopted a lucid scoring technique – the zonal scoring system – and data saturation with an excellent inter-observer agreement ($\kappa = 0.82$, $p < 0.05$) was swiftly attained, justifying that the same can efficiently be utilized to train new residents and interns to promptly read and categorize CXRs, promoting an easy transition into core radiology [21].

In agreement with the available literature, we saw that most patients with CXR scores ≥ 1 had bilateral, peripheral alveolar, and interstitial infiltrates [14,22,23]. We also reported a pleural effusion prevalence of 7.05% according to current reviews [24,25]. Like infiltrates, effusions are prevalent bilaterally, ascribed to the ACE 2-associated cytokine-mediated lung damage [25]. A higher frequency of pleural effusions in the left compared to the right could be attributed to a reporting bias due to a transpicuous right costophrenic window [23,26]. A higher ICXRS was significantly associated with categorical outcomes of ICU admission, intubation, and disease severity. Although mortality was more prevalent in patients with a higher ICXRS, there were minimal deaths to establish

significance (4.44%). There was no statistical significance between age and a higher ICXRS. This may be due to an observation that younger patients present to the hospital in later stages of the disease, wherein widespread lung infiltrates are frequent [13,27]. A higher proportion of patients had an ICXRS of 0 at admission (54.19%), although an ICXRS ≥ 4 was strongly predictive of ICU admission and intubation. Cut-off scores for mild and severe disease were established at ≤ 1 and ≥4, respectively. The cut-off score for ICU admission was ≥ 3, and for intubation it was ≥ 4. The study by Toussie *et al.* established low sensitivity and specificity with cut-off scores of ≥ 3 for intubation (sensitivity = 68% and specificity = 67%); on the other hand, our study was performed on almost twice the sample size (388 vs. 751) and established a good area under the curve (AUC), sensitivity – 87.61%, and specificity – 72.90%.

Concerning comorbidities, the study highlights the unfortunate reality that comorbidities such as T2DM, HTN, obesity, OSA, and dyslipidaemia, formerly at a low prevalence in India, are now on an increasing trend [28-30]. Hypothyroidism was reported at 5.59%, but its significance regarding ICXRSs and categorical outcomes could not be established. The former comorbidities along with CKD and previous history of treated Tb had an OR of >1 for a higher ICXRS, ICU admission, and intubation, in line with the scarcely available studies [13,14,31]. It is understood that even in an age-restricted population, the presence of comorbidities can act as a factor pushing COVID-19 over an edge of increased severity and the need for intubation [32].

The primary limitation of this study is its retrospective and selective nature, because CXRs taken at admission prompt physicians to pre-emptively shift patients to the ICU [33]. The analysis was also performed at a referral hospital where a large number of patients are already at a later stage of disease and have been referred from surrounding centres in need of ICU facilities, causing a Berkson bias [18]. The second pandemic wave proved more hazardous, with a higher prevalence of patients with severe disease [34]. The delta variant, predominant during the second wave, was also shown to have quicker and graver CXR features [35]. Another limitation was that CXRs performed via a portable CXR machine with a hybrid analogue added to disparities in patient positing, movement, and rotation; artifacts attained could add confounding variables in assessing ICXRSs [36].

Conclusions

Despite limitations, we have adequately validated ICXRSs for the categorization and prognosis of patients with COVID-19 and effectively studied the effect of comorbidities on ICXRS. Radiological scoring has been consistently proven to improve timeliness and unequivocal reporting [6,37]. According to current literature, this is the first study of its kind in a low resource setting, providing meticulous data and cut-offs for the Zonal Scoring System and investigating the effect of comorbidities on them. We propose that this scoring system be used in primary, community, and tertiary healthcare centres not only for the above but also to maintain radiological and clinical records, track patient progression, and act as a measure of quality improvement in healthcare. Furthermore, we encourage the use of imaging and clinical data via machine learning techniques to help pre-emptively predict ICXRSs and the prognosis of patients with a set of known comorbidities [38].

Acknowledgements

Sincere thanks to Naman Antony, B.E, IISc, Bangalore, India for his contributions to statistical analysis and manuscript formatting, and Rohan James, M.S, University of Columbia, New York, USA for his assistance in resolving technical and grammatical errors.

Disclosure

The authors report no conflicts of interest.

References

1. Rothan HA, Byrareddy SN. The epidemiology and pathogenesis of coronavirus disease (COVID-19) outbreak. J Autoimmun 2020; 109: 102433. doi: 10.1016/j.jaut.2020.102433.
2. Callaway E. Beyond Omicron: what's next for COVID's viral evolution. Nature 2021; 600: 204-207.
3. Wu Z, McGoogan JM. Characteristics of and important lessons from the coronavirus disease 2019 (COVID-19) outbreak in China: summary of a report of 72 314 cases from the Chinese Center for Disease Control and Prevention. JAMA 2020; 323: 1239-1242.
4. Katzourakis A. COVID-19: endemic doesn't mean harmless. Nature 2022; 601: 485. doi: 10.1038/d41586-022-00155-x.
5. Zhang Y, Xue H, Wang M, et al. Lung ultrasound findings in patients with coronavirus disease (COVID-19). Am J Roentgenol 2021; 216: 80-84.
6. Schiaffino S, Tritella S, Cozzi A, et al. Diagnostic performance of chest X-Ray for COVID-19 pneumonia during the SARS-CoV-2 pandemic in Lombardy, Italy. J Thorac Imaging 2020; 35: W105-W106.
7. Hani C, Trieu NH, Saab I, et al. COVID-19 pneumonia: a review of typical CT findings and differential diagnosis. Diagn Interv Imaging 2020; 101: 263-268.
8. Yasin R, Gouda W. Chest X-ray findings monitoring COVID-19 disease course and severity. Egypt J Radiol Nucl Med 2020; 51: 193. doi: 10.1186/s43055-020-00296-x

9. Bernheim A, Mei X, Huang M, et al. Chest CT findings in coronavirus disease-19 (COVID-19): relationship to duration of infection. Radiology 2020; 295: 200463. doi: 10.1148/radiol.2020200463.
10. Benmalek E, Elmhamdi J, Jilbab A. Comparing CT scan and chest X-ray imaging for COVID-19 diagnosis. Biomed Eng Adv 2021; 1: 100003. doi: 10.1016/j.bea.2021.100003.
11. Sverzellati N, Ryerson CJ, Milanese G, et al. Chest x-ray or CT for COVID-19 pneumonia? Comparative study in a simulated triage setting. Eur Respir J 2021. doi: 10.1183/13993003.04188-2020.
12. ACR Recommendations for the use of Chest Radiography and Computed Tomography (CT) for Suspected COVID-19 Infection [Internet]. [cited 2022 May 18]. Available from: https://www.acr.org/Advocacy-and-Economics/ACR-Position-Statements/Recommendations-for-Chest-Radiography-and-CT-for-Suspected-COVID19-Infection.
13. Kaleemi R, Hilal K, Arshad A, et al. The association of chest radiographic findings and severity scoring with clinical outcomes in patients with COVID-19 presenting to the emergency department of a tertiary care hospital in Pakistan. PLoS One 2021; 16: e0244886. doi: 10.1371/journal.pone.0244886.
14. Toussie D, Voutsinas N, Finkelstein M, et al. Clinical and chest radiography features determine patient outcomes in young and middle-aged adults with COVID-19. Radiology 2020; 297: E197-206.
15. Warren MA, Zhao Z, Koyama T, et al. Severity scoring of lung oedema on the chest radiograph is associated with clinical outcomes in ARDS. Thorax 2018; 73: 840-846.
16. Borghesi A, Maroldi R. COVID-19 outbreak in Italy: experimental chest X-ray scoring system for quantifying and monitoring disease progression. Radiol Med 2020; 125: 509-513.
17. Alqahtani JS, Oyelade T, Aldhahir AM, et al. Prevalence, severity and mortality associated with COPD and smoking in patients with COVID-19: a rapid systematic review and meta-analysis. PLoS One 2020; 15: e0233147. doi: 10.1371/journal.pone.0233147.
18. Westreich D. Berkson's bias, selection bias, and missing data. Epidemiology 2012; 23: 159-164.
19. Jazieh AR, Kozlakidis Z. Healthcare transformation in the post-coronavirus pandemic era. Front Med (Lausanne) 2020; 7: 429. doi: 10.3389/fmed.2020.00429.
20. Sailer AM, van Zwam WH, Wildberger JE, Grutters JPC. Cost-effectiveness modelling in diagnostic imaging: a stepwise approach. Eur Radiol 2015; 25: 3629-3637.
21. Vaughan L, McAlister G, Bell D. 'August is always a nightmare': results of the Royal College of Physicians of Edinburgh and Society of Acute Medicine August transition survey. Clin Med 2011; 11: 322-326.
22. Shi H, Han X, Jiang N, et al. Radiological findings from 81 patients with COVID-19 pneumonia in Wuhan, China: a descriptive study. Lancet Infect Dis 2020; 20: 425-434.
23. Colman J, Zamfir G, Sheehan F, et al. Chest radiograph characteristics in COVID-19 infection and their association with survival. Eur J Radiol Open 2021; 8: 100360. doi: 10.1016/j.ejro.2021.100360.
24. Chong WH, Saha BK, Conuel E, Chopra A. The incidence of pleural effusion in COVID-19 pneumonia: state-of-the-art review. Heart Lung 2021; 50: 481-490.
25. Rathore SS, Hussain N, Manju AH, et al. Prevalence and clinical outcomes of pleural effusion in COVID-19 patients: a systematic review and meta-analysis. J Med Virol 2022; 94: 229-239.
26. Hooper C, Lee YCG, Maskell N. Investigation of a unilateral pleural effusion in adults: British Thoracic Society pleural disease guideline 2010. Thorax 2010; 65 (Suppl 2): ii4-17.
27. Cunningham JW, Vaduganathan M, Claggett BL, et al. Clinical outcomes in young US adults hospitalized with COVID-19. JAMA Intern Med 2020; 181: 379-381.
28. Luhar S, Timæus IM, Jones R, et al. Forecasting the prevalence of overweight and obesity in India to 2040. PLoS One 2020; 15: e0229438. doi: 10.1371/journal.pone.0229438.
29. Gupta R, Gaur K, S. Ram CV. Emerging trends in hypertension epidemiology in India. J Hum Hypertens 2019; 33: 575-587.
30. Pradeepa R, Mohan V. Epidemiology of type 2 diabetes in India. Indian J Ophthalmol 2021; 69: 2932-2938.
31. Gao Y, Liu M, Chen Y, et al. Association between tuberculosis and COVID-19 severity and mortality: a rapid systematic review and meta-analysis. J Med Virol 2021; 93: 194-196.
32. Lighter J, Phillips M, Hochman S, et al. Obesity in patients younger than 60 years is a risk factor for COVID-19 hospital admission. Clin Infect Dis 2020; 71: 896-897.
33. Kim HW, Capaccione KM, Li G, et al. The role of initial chest X-ray in triaging patients with suspected COVID-19 during the pandemic. Emerg Radiol 2020; 27: 617-621.
34. Jain VK, Iyengar Karthikeyan P, Vaishya R. Differences between first wave and second wave of COVID-19 in India. Diabetes Metab Syndr 2021; 15: 1047-1048.
35. Brakohiapa EKK, Sarkodie BD, Botwe BO, et al. Comparing radiological presentations of first and second strains of COVID-19 infections in a low-resource country. Heliyon 2021; 7: e07818. doi: 10.1016/j.heliyon.2021.e07818.
36. Brady Z, Scoullar H, Grinsted B, et al. Technique, radiation safety and image quality for chest X-ray imaging through glass and in mobile settings during the COVID-19 pandemic. Phys Eng Sci Med 2020; 43: 765-779.
37. Boini S, Guillemin F. Radiographic scoring methods as outcome measures in rheumatoid arthritis: properties and advantages. Ann Rheum Dis 2001; 60: 817-827.
38. Podder P, Mondal MRH. Machine learning to predict COVID-19 and ICU requirement. In: 2020 11th International Conference on Electrical and Computer Engineering (ICECE); 2020, p. 483-486.